Full symmetry, optical activity, and potentials of single-wall and multiwall nanotubes

M. Damnjanović,* I. Milošević, T. Vuković and R. Sredanović
Faculty of Physics, University of Beograd, POB 368, Beograd 11001, Yugoslavia
(Received 8 January 1999)

The full symmetry groups for all single-wall and multiwall carbon nanotubes are found. As for the single-wall tubes, the symmetries form non-Abelian nonsymorphic line groups, enlarging the groups reported in the literature. In the multiwall case, any type of line and axial point groups can be obtained, depending on single-wall constituents and their relative position. The isogonal symmetry is related to the macroscopic tensor properties of the nanotubes. The optical activity is studied within this framework, and a detailed classification of the possible nanotube-based optical devices is given. At the microscopic level, full symmetry is used to find general forms of the characteristic functions of the nanotubes. In particular, the stability of the double-wall configurations and the possibility of chiral currents are discussed. Several other consequences are discussed: quantum numbers and related selection rules, phonon spectra, etc. In particular, the bands of the zigzag and the armchair tubes are generally expected to be fourfold degenerate. [S0163-1829(99)06427-9]

I. INTRODUCTION

Single-wall carbon nanotubes are quasi-one-dimensional (1D) cylindrical structures,[1–3] which can be imagined as rolled up cylinders of the 2D honeycomb lattice of the single atomic layer of crystalline graphite. Frequently, several single-wall tubes are coaxially arranged, forming a multiwall nanotube. Since their diameters are small (down to 0.7 nm) in comparison to their lengths (up to tens of μm), the theoretical model of the extended (i.e., infinite, and hence without caps at the ends) nanotube is well justified.

The symmetry of the nanotubes is relevant both for deep insight into the physical properties (quantum numbers, selection rules, optical activity, conducting properties, etc.) and to simplify calculations. As for single-wall tubes, symmetry studies started with the classification of the graphene tubes according to fivefold, threefold, or twofold axes of the related C_{60} molecule,[4] and gave just a part of their point-group symmetry. The translational periodicity was discussed in the context of the nanotube metallic properties.[5] Finally, the helical and rotational symmetries were found[6,7]: the screw axis was characterized in terms of tube parameters, as well as the order of the principal rotational axis.[7] The first goal of this paper is to complete this task, giving the full geometric symmetry of the extended single-wall nanotubes. Due to their 1D translational periodicity, the resulting groups are the line groups;[8,9] it appears that only two line-group families are relevant: the fifth for the chiral, and the 13th for the armchair and zigzag nanotubes.

The symmetry of the double-wall and multiwall tubes has never been seriously studied, despite their importance for applications in nanodevices. Here we present an exhaustive list of symmetries of such tubes. Depending on the single-wall constituents, and their relative arrangement, the resulting nanotube symmetry may be either a line group or an axial point group.

In Sec. II, at first the necessary notions on the line groups are briefly summarized, and the relevant notation is introduced. Then, in Sec. II A, the line groups of all the nanotubes are derived: the familiar symmetries of the original graphene lattice are transferred into the tubular geometry, and those which remain symmetries of the rolled up lattice form the corresponding line group. In addition to the rotational, translational, and helical symmetries, the horizontal axes and (for zigzag and armchair tubes) mirror and glide planes are also present. The symmetry groups of multiwall nanotubes are studied in Sec. II B. Note that among these there are also tubes that are not translationally periodic.

Many of the physical properties of the nanotubes are determined by their symmetry. First, for the properties characterized by the second-rank tensors (the general form of these tensors has been already found[10]), a detailed analysis is enabled. The study of the optical activity, presented in Sec. III, yields an exhaustive list of the different types of optical activities of the nanotubes, with the optical axes and corresponding examples. These results might be a hint of the experimental setups in the context of the optical nanodevices. Further, the potentials for various physical problems may be modeled with the use of symmetry. The general forms of such potentials are derived in Sec. IV; these are applied in a discussion of the relative positions of the components in the multiwall tubes and the structure of the local current density. Some other related results are discussed in Sec. V.

II. SYMMETRY OF NANOTUBES

The line groups[8,11] contain all symmetries of the systems periodical in one direction, and usually are used in the context of stereoregular polymers and quasi-1D subsystems of 3D crystals. It immediately follows that, being periodic along its axis, any extended single-wall nanotube has the symmetry described by one of the line groups.

All the line-group transformations leave the tube axis (z axis, by convention) invariant. Consequently, such a transformation $(P|t)$ (Koster-Seitz symbol) is some point-group operation P preserving the z axis, followed by the translation for t along the z axis. Action on the point $\mathbf{r}=(x,y,z)$ gives $(P|t)\mathbf{r}=(x',y',z')$, with

$$x'=P_{xx}x+P_{xy}y, \quad y'=P_{yx}x+P_{yy}y, \quad z'=P_{zz}z+t. \qquad (1)$$

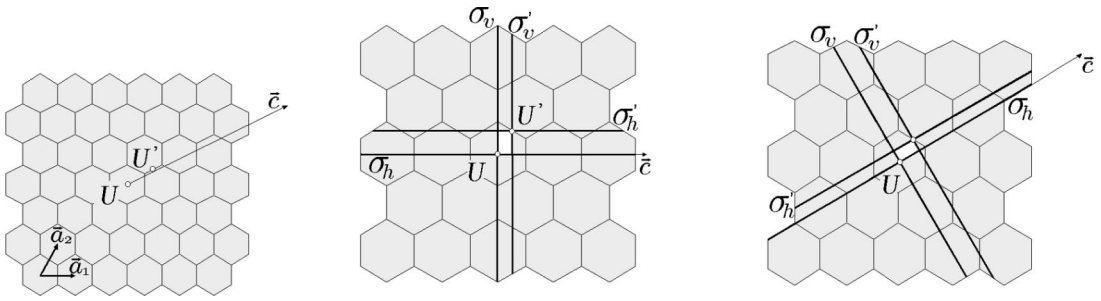

FIG. 1. Symmetries of the honeycomb lattice. For the chiral (8,6), zigzag (6,0), and armchair (6,6) tubes the chiral vectors $\vec{c}$ are depicted by the arrows. The U and U' axes pass through the circles (perpendicular to the honeycomb). In the zigzag and armchair cases, the bold lines σ_v and σ_v' represent the vertical mirror and glide planes of the lattice, being orthogonal to $\vec{c}$; the planes parallel to $\vec{c}$ are denoted as σ_h and σ_h'; U is the intersection of the mirror planes, and U' that of the glide planes.

Here, P_{ij} are elements of the 3×3 matrix of P in the Cartesian coordinates; those coupling z to the other axes vanish. Such point operations are called axial, and they form seven types of the axial point groups:[12] $\mathbf{C}_n$, $\mathbf{S}_{2n}$, $\mathbf{C}_{nh}$, $\mathbf{C}_{nv}$, $\mathbf{D}_n$, $\mathbf{D}_{nd}$, and $\mathbf{D}_{nh}$, where $n=1,2,\ldots$ is the order of the principal rotational axis.

There are infinitely many line groups, since there is no crystallographic restriction on the order of the principal axis, and they are classified within 13 families. Each line group is a product $\mathbf{L}=\mathbf{ZP}$ of one axial point group $\mathbf{P}$ and one infinite cyclic group $\mathbf{Z}$ of generalized translations (screw axis $\mathbf{T}_q^r$, pure translations $\mathbf{T}=\mathbf{T}_1^0$, or glide plane $\mathbf{T}_c$, generated by the transformations $(C_q^r|(n/q)a)$, $(I|a)$, and $(\sigma_v|a/2)$, respectively,[13]). Thus, to determine the full symmetry of a nanotube, both of these factors (having only the identical transformation in common) should be found. The point factor $\mathbf{P}$ should be distinguished from the isogonal point group $\mathbf{P}_I$ of the line group:[11] only for the symorphic groups when $\mathbf{Z}=\mathbf{T}$, these groups are equal; otherwise $\mathbf{P}_I$ is not a subgroup of $\mathbf{L}$. Due to the convention,[13] $2\pi/q$ is the minimal angle of rotation performed by the elements of the line group (if the screw axis is nontrivial it is followed by some fractional translation), as well as by its isogonal point group.

The easiest way to determine the line group $\mathbf{L}$ of a system is first to find the subgroup $\mathbf{L}^{(1)}$, containing all the translations and the rotations around the principal axis (including the ones followed by fractional translations). Having the same screw axis ($\mathbf{T}$ is a special case) as $\mathbf{L}$, and the same order n of the principal axis, this subgroup $\mathbf{L}^{(1)}=\mathbf{T}_q^r\mathbf{C}_n$ is the maximal subgroup from the first line-group family. Then the symmetries complementing $\mathbf{L}^{(1)}$ to $\mathbf{L}$ should be looked for. To complete $\mathbf{Z}$, it should be checked if there is a vertical glide plane. Also, $\mathbf{C}_n$ is to be complemented to $\mathbf{P}$ by eventual additional point-group generators; at most two of them are to be chosen among the mirror planes, horizontal rotational axes of order 2 or rotoreflection axis (refining pure rotations that are already encountered in $\mathbf{C}_n$).

A. Single-wall nanotubes

Elementary cell of the hexagonal honeycomb lattice (Fig. 1) is formed by vectors $\vec{a}_1$ and $\vec{a}_2$ of the length $a_0=2.461$ Å; within its area $S_g=\sqrt{3}/2a_0^2$ there are two carbon atoms at positions $(\vec{a}_1+\vec{a}_2)/3$ and $2(\vec{a}_1+\vec{a}_2)/3$. The single-wall nanotube (n_1,n_2) is formed when the honeycomb lattice is rolled up in such a way that the chiral vector $\vec{c}=n_1\vec{a}_1+n_2\vec{a}_2$ becomes the circumference of the tube (its end and origin match). The tubes $(n_1,0)$ and (n_1,n_1) are called zigzag and armchair tubes, respectively, while the others are known as chiral tubes. The chiral angle θ of the nanotube is the angle between the chiral vector $\vec{c}$ and the zigzag direction $\vec{a}_1$. When $0\leqslant\theta<\pi/3$, all the tubes are encountered; in fact, for the zigzag and armchair nanotubes θ equals 0 and $\pi/6$, respectively, and between these chiralities lay chiral vectors of all the chiral nanotubes with $n_1>n_2>0$ [the tubes (n_2,n_1), with $\pi/6<\theta<\pi/3$, are their optical isomers, as will be discussed later].

There are $n=\mathcal{G}(n_1,n_2)$ ($\mathcal{G}$ is the greatest common divisor) honeycomb lattice points laying on the chiral vector. The translations for $s\vec{c}/n$ in the chiral direction on the tube appear as the rotations for $2s\pi/n$ $(s=0,1,\ldots)$ around the tube axis. Thus the principal axis of order n is a subgroup of the full symmetry of the tube (n_1,n_2):

$$\mathbf{C}_n, \quad n=\mathcal{G}(n_1,n_2). \tag{2}$$

Obviously, $n=n_1$ for the zigzag $(n_1,0)$ and armchair (n_1,n_1) nanotubes.

To the primitive translation of the tube corresponds the vector $\vec{a}=a_1\vec{a}_1+a_2\vec{a}_2$ in the honeycomb lattice, being the minimal one among the lattice vectors orthogonal onto $\vec{c}$. Therefore, a_1 and a_2 are coprimes, yielding

$$\vec{a}=-\frac{2n_2+n_1}{n\mathcal{R}}\vec{a}_1+\frac{2n_1+n_2}{n\mathcal{R}}\vec{a}_2,$$

$$a=|\vec{a}|=\frac{\sqrt{3(n_1^2+n_2^2+n_1n_2)}}{n\mathcal{R}}a_0, \tag{3}$$

with $\mathcal{R}=3$ if $(n_1-n_2)/3n$ is integer and $\mathcal{R}=1$ otherwise. For the zigzag and armchair tubes $a=\sqrt{3}a_0$ and $a=a_0$, respectively. The elementary cell of the tube is the cylinder of the height a and area $S_t=a|\vec{c}|$; it contains $S_t/S_g=2[(n_1^2+n_2^2+n_1n_2/n\mathcal{R}]$ elementary graphene cells.[7] So, the translational group $\mathbf{T}$ of the nanotube is composed of the elements $(I|ta)$, $t=0,\pm1,\ldots$.

The encountered symmetries $\mathbf{T}$ and $\mathbf{C}_n$ originate from the honeycomb lattice translations: on the folded lattice the translations along the chiral vector become pure rotations,

while those along $\vec{a}$ remain pure translations. These elements generate the whole nanotube from the sector of angle $2\pi/n$ of the elementary cell, with $2[(n_1^2+n_2^2+n_1n_2)/n^2\mathcal{R}]$ elementary graphene cells. This number is always greater than 1, pointing out that not all of the honeycomb lattice translations are taken into account. The missing translations are neither parallel with nor orthogonal onto $\vec{c}$; on the rolled up sheet they are manifested as rotations (for fraction of $2\pi/n$) combined with translations (for fractions of a), yielding the screw axis of the nanotube. Its generator $[C_q^r|(n/q)a]$ corresponds to the vector $\vec{z}=r(\vec{c}/q)+n(\vec{a}/q)$ of the honeycomb lattice, which, together with the encountered translations, generates the whole honeycomb lattice. Thus $\vec{z}$ can be chosen to form the elementary honeycomb cell together with the minimal lattice vector $\vec{c}/n$ along the chiral direction. The honeycomb cell area S_g must be the product of $|\vec{c}|/n$ and the length na/q of the projection of $\vec{z}$ onto $\vec{a}$: $a|\vec{c}|/q=\sqrt{3}a_0^2/2$. This gives the order q of the screw axis. Finally, r is found[14] from the condition that projections of $\vec{z}$ on the $\vec{a}_1$ and $\vec{a}_2$ are coprimes. This completely determines the screw axis (Fr$[x]=x-[x]$ is the fractional part of the rational number x, and $\varphi(m)$ is the Euler function, giving the number of coprimes less than m):

$$\mathbf{Z}=\mathbf{T}_q^r, \quad q=2\frac{n_1^2+n_1n_2+n_2^2}{n\mathcal{R}},$$

$$r=\frac{q}{n}\mathrm{Fr}\left[\frac{n}{q\mathcal{R}}\left(3-2\frac{n_1-n_2}{n_1}\right)+\frac{n}{n_1}\left(\frac{n_1-n_2}{n}\right)^{\varphi(n_1/n)-1}\right]. \tag{4}$$

For both the zigzag $(n,0)$ and armchair (n,n) tubes, $q=2n$ and $r=1$, i.e., $\mathbf{Z}=\mathbf{T}_{2n}^1$. Note that q is an even multiple of n. It is equal to the number of the graphene cells in the elementary cell of the tube S_t/S_g. Therefore, q/n is the number of the graphene cells in the sector, and is therefore always greater than 1; this means that all the single-wall tubes have nonsymorphic symmetry groups.

To resume, the translational symmetry of the honeycomb lattice appears as the group $\mathbf{L}^{(1)}=\mathbf{T}_q^r\mathbf{C}_n$ of symmetries of the nanotube, with q and r given by Eqs. (4). Its elements $(C_q^{rt}C_n^s|tn/qa)$ $(t=0,\pm1,\ldots,\ s=0,\ldots,n-1)$ generate the whole nanotube from any adjacent pair of the nanotube atoms. The group $\mathbf{L}^{(1)}$ contains all the symmetries previously considered in the literature.[4,6,7,3] Note that the screw axis used here is somewhat different to the previously reported ones, due to the convention.[13] With this convention $2\pi/q$ is the minimal rotation (followed by some fractional translation) in the group,[14] providing that q is the order of the principal axis of the isogonal point group. This explains why q is equal to the number of graphene cells contained in the elementary cell of the tube. Note that the translational period a and the diameter D of the tube are determined by the symmetry parameters q and n:

$$a=\sqrt{\frac{3q}{2\mathcal{R}n}}a_0, \quad D=\frac{1}{\pi}\sqrt{\frac{\mathcal{R}nq}{2}}a_0. \tag{5}$$

Besides the translations, there are other symmetries of the honeycomb lattice: (a) perpendicular rotational axes through the centers of the hexagons (of order 6), through the carbon atoms (of order 3) and through the centers of the edges of the hexagons (of order 2); (b) six vertical mirror planes through the centers of the hexagons formed by the atoms (or through the atoms); and (c) two types of vertical glide planes—connecting the midpoints of the adjacent edges, and the midpoints of the next to nearest-neighboring edges of the hexagons.

Among the rotations, only those for π, leaving invariant the axis of $\vec{a}$, i.e., the z axis of the tube, remain the symmetry of the rolled up lattice. Thus two types of horizontal second-order axes emerge as symmetries of any nanotube (Fig. 1): U, passing through the center of the deformed nanotube hexagons; and U', passing through the midpoints of the adjacent atoms. Moreover, the first of these transformations is obtained when the second one is followed by the screw axis generator: $U=(C_q^r|(n/q)a)U'$. Thus, any of them, say U, complements the principal tube axis $\mathbf{C}_n$ to the dihedral point group $\mathbf{D}_n$. This shows that at least the line group $\mathbf{T}_q^r\mathbf{D}_n$ (from the fifth family) is the symmetry group of any nanotube. Note that U' just permutes the two carbon atoms in the elementary honeycomb cell, meaning that all the honeycomb atoms are obtained from an arbitrary one by the translations and the rotation U'. Analogously, the elements of the group $\mathbf{T}_q^r\mathbf{D}_n$ generate the whole nanotube from any of its atoms. Action (1) of the group elements on the point $\mathbf{r}_{000}=(\rho_0,\phi_0,z_0)$ (cylindrical coordinates) gives the points

$$\mathbf{r}_{tsu}=\left(C_q^{rt}C_n^sU^u\middle|t\frac{n}{q}a\right)\mathbf{r}_{000}$$
$$=\left[\rho_0,(-1)^u\varphi_0+2\pi\left(\frac{t}{q}+\frac{s}{n}\right),(-1)^uz_0+t\frac{n}{q}a\right], \tag{6}$$

$(u=0,1;\ s=0,\ldots,n-1;\ t=0,\pm1,\ldots)$; hereafter the x axis is assumed to coincide with the U axis. Using Eq. (5), it can be shown that the coordinates of the first atom (positioned at $\frac{1}{3}(\vec{a}_1+\vec{a}_2)$ on the honeycomb) are

$$\mathbf{r}_{000}^C=\left(\frac{D}{2},2\pi\frac{n_1+n_2}{nq\mathcal{R}},\frac{n_1-n_2}{\sqrt{6nq\mathcal{R}}}a_0\right). \tag{7}$$

Substituting these values into Eq. (6), the coordinates of all other atoms are obtained.

Rolling up deforms any plane perpendicular onto the graphene sheet, unless it is either parallel with $\vec{c}$ (then it becomes a horizontal plane) or orthogonal to $\vec{c}$ (giving a vertical plane). Thus only tubes with chiral vectors parallel or orthogonal to the enumerated mirror and glide planes obtain additional symmetries of these types. The zigzag and armchair tubes are immediately singled out by simple inspection. Only in these cases is the chiral vector in a perpendicular mirror plane; when the sheet is rolled up, this plane becomes the horizontal mirror plane σ_h of the corresponding nanotubes. Enlarging the previously found point symmetry group $\mathbf{D}_n$ by σ_h, the point group $\mathbf{D}_{nh}$ of the zigzag and armchair tubes is obtained. Finally, taking into account the generalized translations (4), the full symmetry groups of the

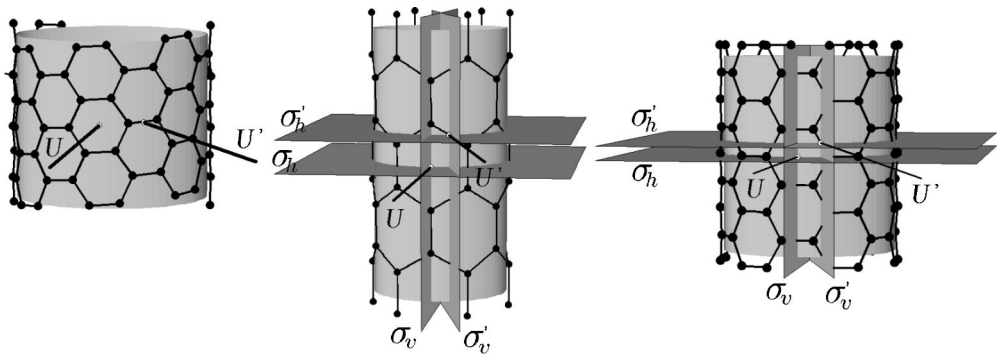

FIG. 2. Symmetries of the single-wall nanotubes: (8,6), (6,0), and (6,6). The horizontal rotational axes U and U' are symmetries of all the tubes, while the mirror planes (σ_v and σ_h), the glide plane σ_v', and the rotoreflectional plane σ_h' are symmetries of the zigzag and armchair tubes only. The line groups are $\mathbf{T}_{148}^{21}\mathbf{D}_2$ for (8,6), and $\mathbf{T}_{12}^{1}\mathbf{D}_{6h}$ for the other two tubes.

single-wall nanotubes are (besides the factorized notation, the international symbol is also given):

$$\mathbf{L}_{\text{chiral}}=\mathbf{T}_q^r\mathbf{D}_n=\mathbf{L}q_p22,$$

$$p=q\text{Fr}\left[\frac{n\mathcal{R}}{q}\frac{\left(\frac{2n_2+n_1}{n\mathcal{R}}\right)^{\varphi(2n_1+n_2/n\mathcal{R})-1}{}^{q-n_2}}{2n_1+n_2}\right], \quad (8a)$$

$$\mathbf{L}_{\text{armchair}}=\mathbf{L}_{\text{zigzag}}=\mathbf{T}_{2n}^1\mathbf{D}_{nh}=\mathbf{L}2n_n/mcm. \quad (8b)$$

Their isogonal point groups[11] are $\mathbf{D}_q$ and $\mathbf{D}_{2nh}$.

The line group $\mathbf{T}_{2n}^1\mathbf{D}_{nh}$ (13th family) contains various new symmetries (Fig. 2), all combinations of the ones mentioned above. In fact, when σ_h has been added to the group $\mathbf{T}_{2n}^1\mathbf{D}_n$, the other mirror and glide planes parallel to and orthogonal onto $\vec{c}$ are automatically included in the symmetry groups of the zigzag and armchair nanotubes. These transformations can be seen as σ_h followed by some of the elements from $\mathbf{T}_{2n}^1\mathbf{D}_n$. At first, there are n vertical mirror planes (one of them is $\sigma_v=\sigma_hU$, and the others are obtained by pure rotations; by the previous convention, the σ_h plane is the xy-coordinate plane). Bisecting the mirror planes, there are glide planes [e.g., the product $(\sigma_v'|\frac{1}{2})=(C_{2n}|\frac{1}{2}a)\sigma_v$], and the vertical rotoreflection axis of order $2n$ (generated by $\sigma_vU'=C_{2n}\sigma_h'$, the reflection in the σ_h' plane, followed by the rotation for π/n).

The vectors obtained from $\vec{c}$ by the rotations from the point symmetry group $\mathbf{C}_{6v}$ of the honeycomb lattice, produce the nanotubes which are essentially the same one, only looked at from the rotated coordinate systems. Nevertheless, the vertical mirror plane image of $\vec{c}$ (e.g., in the vertical plane bisecting the angle of $\vec{a}_1$ and $\vec{a}_2$) produces the tube which can be considered as the same one only in the coordinate system with the opposite sign (the coordinate transformation involves the spatial inversion). Thus tubes (n_1,n_2) and (n_2,n_1) are optical isomers. Only the mirror image of the zigzag and armchair tubes is equivalent to the original, and these tubes have no optical isomers. This is manifested in the optical activity, as will be discussed in sec. III. Concerning the symmetry groups, if $\mathbf{T}_q^r\mathbf{C}_n$ corresponds to the tube (n_1,n_2), then the group of the tube (n_2,n_1) is $\mathbf{T}_q^{(q/n)-r}\mathbf{C}_n$ (although isomorphic, these groups are equal only when $q=2n$ and $r=1$, i.e., only for the zigzag and armchair tubes).

B. Double-wall and multiwall nanotubes

The symmetry of a multiwall nanotube now can be found as intersection of the symmetry groups of its single-wall constituents. This task will be considered for double-wall tubes at first, and then the results are straightforwardly generalized to the multiwall ones. The intersection of the line groups $\mathbf{L}=\mathbf{ZP}$ and $\mathbf{L}'=\mathbf{Z}'\mathbf{P}'$ has the form $\mathbf{L}_2=\mathbf{Z}_2(\mathbf{P}\cap\mathbf{P}')$. Thus the intersection of the point groups is looked for independently of the generalized translations.

As derived in Eq. (2), the tubes (n_1,n_2) and (n_1',n_2') are invariant under the rotations around their axes for the multiples of the angles $2\pi/n$ and $2\pi/n'$ [$n=\mathcal{G}(n_1,n_2)$ and $n'=\mathcal{G}(n_1',n_2')$], respectively. The tube composed of these coaxially arranged components is invariant under the rotation for $2\pi/N$, the minimal common rotation of the components, and its multiples. Thus the principal axis subgroup of the double-wall nanotube is $\mathbf{C}_N$, with $N=\mathcal{G}(n,n')=\mathcal{G}(n_1,n_2,n_1',n_2')$. The horizontal second-order rotational axis U (and U') is also symmetry of all single-wall nanotubes. Nevertheless, such an axis remains the symmetry of the composite tube only if it is common to all of the components, and then the point symmetry is $\mathbf{D}_N$. Obviously, if a nanotube contains at least one chiral component, then $\mathbf{D}_N$ is its maximal point symmetry. Only tubes composed exclusively of zigzag and armchair single-wall components may have additional mirror and glide planes, as well as a rotoreflectional axis. Analogously to the horizontal axis, these are symmetries of the whole tube only if they are common for all of the components (the rotoreflectional axis appear only if the horizontal planes σ_h' coincides).

After the point symmetries are thereby completely determined, the more difficult study of the generalized translational factor $\mathbf{Z}_2$ remains. Note that, at first, it may be completely absent. Suppose that double-wall tube has the translational period A. If the translational periods of its constituents are a and a', then A is obviously the minimal distance being multiple both of a and of a': $A=\alpha a=\alpha' a'$, where α and α' are positive coprimes (to assure minimality). Thus the double-wall tube is translationally periodic if and

TABLE I. Symmetry of the multiwall zigzag and armchair tubes. For the periodic tubes, the line groups (and families) and the isogonal groups are in the ''odd'' columns if all the ratios n/N, n'/N, ... are odd, and in the ''even'' columns otherwise. The point groups of the tubes with both zigzag and armchair components are in the last column. In the first column the relative positions of the component tubes are characterized by the coinciding symmetry elements (beside the common principal axis in the general position). Here (U,U') denotes the horizontal axis, which is the U axis in some of the constituents, and the U' axis in the remaining ones (to exclude the additional mirror or glide planes). Also, (σ_h,σ_h') is the plane, which is σ_h in some of the constituents (with even n, necessarily) and σ_h' in the remaining tubes; in the incommensurate case, the same groups are obtained when σ_h' planes are in common.

Relative position	Line group ''Odd''		Line group ''Even''		Isogonal group ''Odd''	Isogonal group ''Even''	Point group
General	$\mathbf{T}^1_{2N}\mathbf{C}_N$	(1)	$\mathbf{TC}_N$	(1)	$\mathbf{C}_{2N}$	$\mathbf{C}_N$	$\mathbf{C}_N$
σ_h	$\mathbf{T}^1_{2N}\mathbf{C}_{Nh}$	(4)	$\mathbf{TC}_{Nh}$	(3)	$\mathbf{C}_{2Nh}$	$\mathbf{C}_{Nh}$	$\mathbf{C}_{Nh}$
σ_v	$\mathbf{T}^1_{2N}\mathbf{C}_{Nv}$	(8)	$\mathbf{TC}_{Nv}$	(6)	$\mathbf{C}_{2Nv}$	$\mathbf{C}_{Nv}$	$\mathbf{C}_{Nv}$
σ_v'	$\mathbf{T}^1_{2N}\mathbf{C}_{Nv}$	(8)	$\mathbf{T}_c\mathbf{C}_{Nv}$	(7)	$\mathbf{C}_{2Nv}$	$\mathbf{C}_{Nv}$	$\mathbf{C}_N$
(U,U')	$\mathbf{T}^1_{2N}\mathbf{D}_N$	(5)	$\mathbf{TD}_N$	(5)	$\mathbf{D}_{2N}$	$\mathbf{D}_N$	$\mathbf{D}_N$
σ_h,σ_v	$\mathbf{T}^1_{2N}\mathbf{D}_{Nh}$	(13)	$\mathbf{TD}_{Nh}$	(11)	$\mathbf{D}_{2Nh}$	$\mathbf{D}_{Nh}$	$\mathbf{D}_{Nh}$
σ_h,σ_v'	$\mathbf{T}^1_{2N}\mathbf{D}_{Nh}$	(13)	$\mathbf{T}_c\mathbf{C}_{Nh}$	(12)	$\mathbf{D}_{2Nh}$	$\mathbf{D}_{Nh}$	$\mathbf{C}_{Nh}$
(σ_h,σ_h')	$\mathbf{T}^1_{2N}\mathbf{C}_{Nh}$	(4)	$\mathbf{TS}_{2N}$	(2)	$\mathbf{C}_{2Nh}$	$\mathbf{S}_{2N}$	$\mathbf{S}_{2N}$
$(\sigma_h,\sigma_h'),\ \sigma_v$	$\mathbf{T}^1_{2N}\mathbf{D}_{Nh}$	(13)	$\mathbf{TD}_{Nd}$	(9)	$\mathbf{D}_{2Nh}$	$\mathbf{D}_{Nd}$	$\mathbf{D}_{Nd}$
$(\sigma_h,\sigma_h'),\ \sigma_v'$	$\mathbf{T}^1_{2N}\mathbf{D}_{Nh}$	(13)	$\mathbf{T}_c\mathbf{S}_{2N}$	(10)	$\mathbf{D}_{2Nh}$	$\mathbf{D}_{Nd}$	$\mathbf{S}_{2N}$

only if the translational periods of its constituents are commensurate, i.e., only when a'/a is rational. Conversely, if a'/a is an irrational number, the composed tube is not translationally periodic, and $\mathbf{Z}_2$ is trivial (identical transformation only); the total symmetry reduces to the already found point group.

In the commensurate case it remains to examine if the translational group can be refined by a screw axis, common to all of the single-wall components. The task is to determine the screw axis generator $(C_Q^R|F)$ with maximal Q, appearing in the both groups $\mathbf{L}=\mathbf{T}^r_q\mathbf{C}_n$ and $\mathbf{L}'=\mathbf{T}^{r'}_{q'}\mathbf{C}_{n'}$. Thus we look for the values of Q, R and F (in accordance with Ref. 13), such that there exist integers t, s, t', and s' (enumerating the elements of $\mathbf{L}$ and $\mathbf{L}'$) satisfying

$$(C_Q^R|F)=(C_q^{rt}C_n^s|tf)=(C_{q'}^{r't'}C_{n'}^{s'}|t'f')$$

$$\text{with}\quad F=\frac{N}{Q}A, f=\frac{n}{q}a,\quad f'=\frac{n'}{q'}a'. \tag{9}$$

Obviously, the fractional translation F is multiple $F=tF^*$ of the minimal common fractional translation F^*, implying $A=(Q/N)tF^*$. Analogously to A, the translation F^* is found as the minimal distance being multiple both of f and f'; thus it is given by the unique solution in the coprimes ϕ and ϕ' of the equation $F^*=\phi f=\phi' f'$. Since the translational periods of the single-wall components are multiples of their fractional translations, A is multiple of F^*, i.e., $A=\Phi F^*$. With the help of number theory, it can be shown[14] that only the tubes with the same $\mathcal{R}$ may be commensurate; then $\alpha=\phi'=\sqrt{q'/n'\mathcal{G}(q/n,q'/n')}$, $\alpha'=\Phi=\sqrt{q/n/\mathcal{G}(q/n,q'/n')}$ and $\Phi=\sqrt{qq'/nn'}$. Thus $Q=\Phi N/\tau$, and the minimal τ is looked for to provide the finest screw axis. The translational part of Eq. (9) immediately shows that $t=\tau\alpha'$ and $t'=\tau\alpha$. With this value substituted, the rotational part of Eq. (9) gives the equations

$$C_Q^R=C_q^{r\alpha'\tau}C_n^s=C_{q'}^{r'\alpha\tau}C_{n'}^{s'}. \tag{10}$$

The minimal τ for which the last equation is solvable in s and s' is $\tau=\Phi/\mathcal{G}(r\alpha n'/N-r'\alpha' n/N,\Phi)$. Finally, $Q=N\mathcal{G}(r\alpha n'/N-r'\alpha' n/N,\sqrt{qq'/nn'})$, and R is easily found from Eq. (10).

All these results are immediately generalized to the multiwall tubes. Note that the generalized translations and the principal rotational axis of the multiwall nanotube depend only on the types of their single-wall components. Conversely, the appearance of the mirror and glide planes and the horizontal axes in the common symmetry group is additionally determined by the relative positions of these components.

It remains to give the summary of the symmetry groups of the multiwall tubes. If at least one of the single-wall constituents is chiral, then in the commensurate case there are two possibilities: $\mathbf{T}^R_Q\mathbf{C}_N$, corresponding to the general mutual position; and $\mathbf{T}^R_Q\mathbf{D}_N$ in the special mutual positions with common U axis. Analogously, the tube built of incommensurate components has a symmetry described by the point groups $\mathbf{C}_N$ or $\mathbf{D}_N$. If the nanotube is built of zigzag and armchair single-wall tubes $(n,0)$ [or (n,n), $(n',0)$ or (n',n')], ..., the order of the principal rotational axis is $N=\mathcal{G}(n,n',\ldots)$. If the tube contains at least one single-wall tube of both types, no translational periodicity appears and its symmetry is described by a point group (Table I). On the other hand, for a tube composed of components of the same type (either zigzag or armchair), the translational period is equal to that of the components. Two different situations may occur: if all the integers n/N, $n'/N\ldots$ are odd (''odd'' case), the translations are refined by the screw axis $\mathbf{T}^1_{2N}$; otherwise, if at least one of these integers is even (''even'' case), no screw axis emerges. The analysis of the special arrangements of constituents with common horizontal axes, mirror or glide planes, increasing the symmetry of the total system is sum-

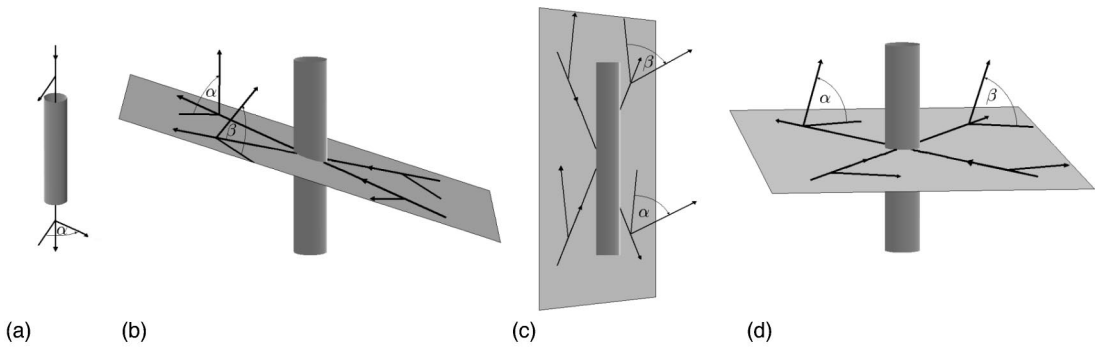

FIG. 3. Optical activity of carbon nanotubes. The optical axes (with the direction of the beams) are indicated by the arrows. For the double-axis devices, the axes' plane is shown; initially, field vectors (arrows orthogonal to the axes) are polarized in this plane. The out-of-plane arrows indicate the rotated (for the angles α and β) field vectors of the outgoing beams. The positions of the axes and the relative values of α and β in (a)–(d) depend on the symmetry group of the tube, and they are specified in the text.

marized in Table I. Note that according to the various arrangements of the components, any of the line and axial point groups may be the resulting symmetry for the commensurate and incommensurate components, respectively. Some examples are given in Sec. III.

III. OPTICAL ACTIVITY

As the symmetry classification of the single-wall and multiwall carbon nanotubes has been completed, the general matrix forms of the symmetrical polar and axial second-rank tensors for systems having line-group symmetry[10] can be used to predict many of the physical properties. Here the optical activity of the isolated carbon nanotubes will be analyzed in order to select the nanotubes relevant for further experiments on optical activity and propose the characteristic experimental setups. To avoid the influence of the other effects, birefringence and anisotropy of absorption, only the activity along the optical axes is discussed (the birefringence in thin films of aligned carbon nanotubes has been already reported[15]). Different types of activity are illustrated by double-wall tubes with a realistic interlayer distance[1,16] of approximately 3.4 Å , giving examples of potentially interesting nano-optical devices; their metallic or semiconductor properties[17] and commensurability are emphasized. Since the optical activity decreases for nanotubes with larger diameter,[19] tubes with diameters up to 3 nm are considered.

In the optically active medium, the polarization plane of a linearly polarized light beam incoming along the optical axis with the ort $\mathbf{k}=(k_x,k_y,k_z)$, is rotated through an angle $\Sigma_{i,j}k_ik_ja_{ij}$ per unit length; a_{ij} are elements of the optical activity tensor A, an axially symmetric second-rank tensor. Thus, from the general axial tensors of the line groups,[10] the symmetric part is to be taken to obtain the form of A. The general form of the dielectric tensor ε, a polar symmetric second-rank tensor, is used to predict the shape of the optical indicatrice and thereby the spatial orientation of the optical axes of a particular nanotube.[18] When two eigenvalues of ε coincide, the indicatrice is rotational ellipsoid and the tube axis is the only optical axis. On the other hand, when all the eigenvalues of ε are different, two optical axes emerge; although their exact spatial directions may be found only after the values of the permeability tensor elements are known, pure symmetry arguments leave only two or three possibilities, and each of them will be discussed. It should be stressed that the most general symmetry-constrained tensor forms are used, but due to some other physical reasons, the tensors may have an even more specific form. For example, the plausible assumption that the tensor ε is determined by the dielectric permeability of the graphite results in the disappearance of additional tensor components. Discussion of this question is postponed to the end of the section, in order to present the most general results, independent of this assumption (thus the derived forms refer generally to the symmetrical second-rank tensors).

A. Single-wall tubes

The general form of the tensors of dielectric permeability and optical activity for the symmetry groups $\mathbf{T}_q^r\mathbf{D}_n$ of the chiral tubes have the same diagonal form (for $q>2$, which refers to the all realistic tubes):

$$\varepsilon=\begin{pmatrix}\varepsilon_{xx} & 0 & 0\\ 0 & \varepsilon_{xx} & 0\\ 0 & 0 & \varepsilon_{zz}\end{pmatrix},\quad A=\begin{pmatrix}a_{xx} & 0 & 0\\ 0 & a_{xx} & 0\\ 0 & 0 & a_{zz}\end{pmatrix}. \tag{11}$$

Since A does not vanish, the chiral tubes are expected to be optically active. Two equal diagonal elements in ε single out the tube axis as the optical axis. The polarization plane is rotated [Fig. 3(a)] through an angle α proportional to a_{zz}; (the highly oscillatory dependence of a_{zz} on the frequency of the external field[19] may be of additional experimental interest). As already mentioned in Sec. II A, the tubes (n_1,n_2) and (n_2,n_1) are the optical isomers (having screw axes of opposite sign) and thus rotate the polarization of incoming field through equal angles but in opposite directions. On the other hand, single-wall zigzag and armchair nanotubes are optically inactive, since their axial tensors vanish.

B. Double-wall tubes

Only a part of multiwall nanotubes has symmetries (derived in Sec. II A) compatible with the optical activity; these cases will be analyzed and illustrated here. In general positions, the symmetry group of a double-wall tube belongs either to the first line-group family (when the translational periods of the constituents are commensurate) or to the rota-

tional group family $\mathbf{C}_N$ (when the periods are incommensurate). In both cases the optical activity is not forbidden by symmetry. Still, it can be prevented by increased symmetry in the special spatial arrangements of the single-wall constituents. The additional horizontal axes cannot cause this effect and therefore, tubes with at least one chiral component, i.e., chiral-chiral (CC), chiral-armchair (CA), and chiral-zigzag (CZ) components are always active and have optical isomers. Only the zigzag-zigzag (ZZ), armchair-armchair (AA), and armchair-zigzag (AZ) components lose activity when their single-wall constituents are in relative positions with coinciding mirror or glide planes. Otherwise, these tubes may be active, despite the inactivity of their components and the absence of the optical isomers. In addition to this general result, a more subtle discussion on the spatial position of the optical axes is performed. To this end, three classes of nanotubes (differing by the order of the rotational and screw axis) are considered separately, at first in a general position and then in different special positions.

Let us first consider optically active tubes without rotational symmetry; this includes the tubes having in general position either the pure translational symmetry **T** (commensurate constituents; e.g., ZZ and AA, with nn' even and $N=1$), or the trivial group $\mathbf{C}_1$ (incommensurate components; e.g., AZ with $N=1$). Realistic metallic-metallic pairs are AA (6,6)–(11,11), (7,7)–(12,12), CA (11,2)–(12,12), and CC (22,4)–(26,11) (commensurate) and ZA (9,0)–(10,10), (15,0)–(14,14), CZ (11,2)–(21,0), CA (13,4)–(14,14), and CC (10,4)–(19,4) (incommensurate). The commensurate semiconducting-semiconducting nano-optic devices belonging to this class are the ZZ pairs (10,0)–(19,0) and (11,0)–(20,0) and the CC pair (7,3)–(14,6), while the incommensurate ones are the CC pair (6,4)–(17,1), the CZ pair (9,2)–(19,0), and the ZC pair (10,0)–(17,3). Examples of the incommensurate metallic-semiconducting optically active double-wall tubes, belonging to this class, are the AZ pairs (5,5)–(17,0), (6,6)–(19,0), and (8,8)–(23,0), the CC pair (24,9)–(35,6), the CZ pair (25,7)–(38,0), the ZC pair (27,0)–(31,8), and the AC pair (17,17)–(30,13), while the CC pair (21,9)–(28,12) is an example of the commensurate metallic-semiconducting optically active tube. Finally, the incommensurate semiconducting-metallic devices are the ZA-type pairs: (10,0)–(11,11), (14,0)–(13,13), (17,0)–(15,15), the CC pair (6,4)–(13,7), the CZ pair (8,6)–(21,0), the ZC pair (10,0)–(15,6), and the CA pair (16,2)–(15,15), while the commensurate one is the double-wall tube of CC type, (14,6)–(21,9).

To the **T** and $\mathbf{C}_1$ groups correspond the most general forms of the tensors ε and A:

$$\varepsilon=\begin{pmatrix}\varepsilon_{xx}&\varepsilon_{xy}&\varepsilon_{xz}\\ \varepsilon_{xy}&\varepsilon_{yy}&\varepsilon_{yz}\\ \varepsilon_{xz}&\varepsilon_{yz}&\varepsilon_{zz}\end{pmatrix},\quad A=\begin{pmatrix}a_{xx}&a_{xy}&a_{xz}\\ a_{xy}&a_{yy}&a_{yz}\\ a_{xz}&a_{yz}&a_{zz}\end{pmatrix}. \tag{12}$$

Obviously, such systems may be optically active and have two optical axes.

In the special positions in which these pairs of tubes share a horizontal axis (assumed to be the x axis) and neither mirror nor glide planes, the composite tube has the symmetry $\mathbf{TD}_1$ when translational periods are commensurate and only $\mathbf{D}_1$ symmetry, otherwise. The tensor forms are

$$\varepsilon=\begin{pmatrix}\varepsilon_{xx}&0&0\\ 0&\varepsilon_{yy}&\varepsilon_{yz}\\ 0&\varepsilon_{yz}&\varepsilon_{zz}\end{pmatrix},\quad A=\begin{pmatrix}a_{xx}&0&0\\ 0&a_{yy}&a_{yz}\\ 0&a_{yz}&a_{zz}\end{pmatrix}. \tag{13}$$

The system has two optical axes and two situations are possible: either the axes are bisected by the yz plane [Fig. 3(b) for $\alpha=\beta$] when the polarization of beams along them is rotated through the same angles (and in the same directions), or the axes are in the yz plane when the rotations are expected, in general, to be different [Fig. 3(c) for independent α and β].

If the considered tubes are in a special position with a preserved vertical mirror σ_v or glide plane $(\sigma_v'|\frac{1}{2})$ (this excludes the tubes with chiral components) the corresponding symmetry groups are $\mathbf{TC}_{1v}$ (containing a mirror plane) or $\mathbf{T}_c\mathbf{C}_1$ (containing a glide plane) in the translationally periodic case, and $\mathbf{C}_{1v}$ when the components are incommensurate. In all these cases the relevant tensors are of the form (where the xz plane has been taken as the symmetry plane)

$$\varepsilon=\begin{pmatrix}\varepsilon_{xx}&0&\varepsilon_{xz}\\ 0&\varepsilon_{yy}&0\\ \varepsilon_{xz}&0&\varepsilon_{zz}\end{pmatrix},\quad A=\begin{pmatrix}0&a_{xy}&0\\ a_{xy}&0&a_{yz}\\ 0&a_{yz}&0\end{pmatrix}. \tag{14}$$

Analogously, when the horizontal mirror planes coincide, the same pairs have either $\mathbf{TC}_{1h}$ (if commensurate) or $\mathbf{C}_{1h}$ (if incommensurate) symmetry. The general tensor forms are

$$\varepsilon=\begin{pmatrix}\varepsilon_{xx}&\varepsilon_{xy}&0\\ \varepsilon_{xy}&\varepsilon_{yy}&0\\ 0&0&\varepsilon_{zz}\end{pmatrix},\quad A=\begin{pmatrix}0&0&a_{xz}\\ 0&0&a_{yz}\\ a_{xz}&a_{yz}&0\end{pmatrix}. \tag{15}$$

The form of the ε in Eqs. (14) and (15) allows two possibilities for the positions of the optical axes (this depends on the concrete values ε_{ij}): either both of them are in the symmetry plane, or this plane bisects the angle between the optical axes. It is easy to see that only in the second case can the tubes be optically active: if, for the beam incoming along one of the axes, the rotation of the polarization is clockwise, it will be counterclockwise through an equal angle for the beam incoming along the other axis [see Fig. 3(b) for a tube with σ_v symmetry, and Fig. 3(c) for a tube with σ_h symmetry, both with $\beta=-\alpha$].

Finally, when the pairs preserve both horizontal and vertical mirror or glide planes, their symmetry group is $\mathbf{TD}_{1h}$ or $\mathbf{T}_c\mathbf{C}_{1h}$ for ZZ and AA pairs, and $\mathbf{D}_{1h}$ for ZA pairs. All of them have tensors of the following forms:

$$\varepsilon=\begin{pmatrix}\varepsilon_{xx}&0&0\\ 0&\varepsilon_{yy}&0\\ 0&0&\varepsilon_{zz}\end{pmatrix},\quad A=\begin{pmatrix}0&0&0\\ 0&0&a_{yz}\\ 0&a_{yz}&0\end{pmatrix}. \tag{16}$$

Again, there are two optical axes in one of the coordinate planes. The optical activity can be seen only if the axes are in the yz plane. In this case the plane of polarization of two light beams striking the tube along two optical axes will be rotated through equal angles (proportional to a_{yz}) but in the opposite directions [Fig. 3(c), with $\alpha=-\beta$].

To the second class of double-wall nanodevices belong tubes with an order 2 principal axis of the isogonal group.

There are tubes having a screw axis $\mathbf{T}_2^1$ (AA and ZZ pairs for $N=1$, with nn' odd), and tubes with no screw axis but with a second-order principal axis: they may be commensurate (like AA and ZZ pairs for $N=2$ and $nn'/4$ being even) or not (like AZ pairs for $N=2$). Examples of such commensurate metallic-semiconducting pairs are the ZZ pair (9,0)–(17,0) and the CC pair (9,6)–(15,10), while the AZ pair (8,8)–(22,0), the CC pair (12,6)–(18,10), the CZ pair (8,14)–(28,0), and the AC pair (6,6)–(12,10) are examples of the incommensurate devices of the same type. The ZZ pair (13,0)–(21,0) and the CC pair (12,8)–(18,12) are of commensurate semiconducting-metallic type, while incommensurate examples are the ZA tube (16,0)–(14,14), the CC tube (22,12)–(28,16), the CZ tube (16,8)–(30,0), and the ZC tube (14,0)–(16,10). In addition to the AA pairs (always metallic-metallic and commensurate tubes) (5,5)–(9,9) and (7,7)–(11,11), the semiconducting-semiconducting commensurate tubes ZZ (11,0)–(19,0) and CC (6,4)–(12,8) also belong to this class of nano-optic devices. Incommensurate semiconducting-semiconducting devices are the CC pair (10,8)–(16,12), the CZ pair (10,2)–(20,0) and the ZC pair (26,0)–(30,8), while the incommensurate metallic-metallic ones are the CC tube (22,4)–(22,16), the CZ tube (8,2)–(18,0), and the AC tube (8,8)–(16,10).

Generally, the symmetry groups of the considered cases are $\mathbf{T}_2^1\mathbf{C}_1$, $\mathbf{TC}_2$, and $\mathbf{C}_2$. The tensor of the permeability and the consequent geometry of the optical axes are given by ε in Eq. (15). The optical activity tensor has the form

$$A=\begin{pmatrix} a_{xx} & a_{xy} & 0 \\ a_{xy} & a_{yy} & 0 \\ 0 & 0 & a_{zz} \end{pmatrix}. \tag{17}$$

When the both optical axes lie in the xy plane the polarizations of the beams parallel to them is rotated through different angles [Fig. 3(c), with $\alpha\neq\beta$]. Otherwise, the xy plane bisects the axes and the optical activity will be exhibited equally along the axes [Fig. 3(c), with $\alpha=\beta$].

In the special positions of the coaxial single-wall components, preserving the horizontal U axis, the symmetry groups of the above enumerated double-wall tubes are $\mathbf{T}_2^1\mathbf{D}_1$, $\mathbf{TD}_2$ and $\mathbf{D}_2$, respectively. Tensor ε is given by Eq. (16), while

$$A=\begin{pmatrix} a_{xx} & 0 & 0 \\ 0 & a_{yy} & 0 \\ 0 & 0 & a_{zz} \end{pmatrix}. \tag{18}$$

Two optical axes are allowed, and both of them lie in one of the coordinate planes, depending on the values of ε_{xx}, ε_{yy}, and ε_{zz}. The polarization will be rotated through the same angle and with the same sense along the both axes [Figs. 3(c) and 3(d) for $\alpha=\beta$].

In the special position with a common vertical mirror or glide plane, the mentioned ZZ and AA tubes increase the symmetry to $\mathbf{T}_2^1\mathbf{C}_{1v}$, $\mathbf{T}_c\mathbf{C}_2$ or $\mathbf{TC}_{2v}$, and the ZA tubes to $\mathbf{C}_{2v}$. In these cases the permeability tensor is also given by Eq. (16), while the optical tensor has the form

$$A=\begin{pmatrix} 0 & a_{xy} & 0 \\ a_{xy} & 0 & 0 \\ 0 & 0 & 0 \end{pmatrix}. \tag{19}$$

The possible positions of the optical axes are discussed after relation (16), but the activity is allowed only when the axes are in the xy direction: the polarization of the light incoming along the axes is rotated through the same angles but in the opposite sense [Fig. 3(d), with $\alpha=-\beta$].

The third class of double-wall tubes is those for which either Q or N is greater than 2. As for ZZ, AA, and ZA tubes, this means that $N>2$ (also AA and ZZ with $N=2$ if $nn'/4$ is odd). Commensurate metallic-metallic nano-optical devices of this class are the AA pairs (5,5)–(10,10) and (8,8)–(12,12) and the ZZ pairs (9,0)–(18,0) and (12,0)–(21,0), while the incommensurate ones are the AZ pairs (7,7)–(21,0) and (9,9)–(24,0), the ZA pairs (12,0)–(12,12) and (18,0)–(15,15), the CC pair (9,3)–(18,3), the CZ pair (12,9)–(27,0), the ZC pair (15,0)–(18,9), and the CA pair (24,6)–(21,21). The AZ pair (15,15)–(35,0) and the pair ZC (24,0)–(28,8) are examples of the incommensurate metallic-semiconducting double-wall optical devices, the ZA tubes (11,0)–(11,11) and (13,0)–(13,13), the CC tube (20,12)–(32,8), and the ZC tube (28,0)–(32,8) are incommensurate semiconducting-metallic optical devices, and the ZZ pair (10,0)–(18,0) is a commensurate example of the same type. Tube ZZ (14,0)–(22,0) is an example of a commensurate semiconducting-semiconducting system.

In general, for all systems the symmetry position belongs to one of the groups $\mathbf{T}_Q^R\mathbf{C}_N$, $\mathbf{TC}_N$, or $\mathbf{C}_N$. All these cases are characterized by the diagonal tensors ε and A, given by Eq. (11). The only special position allowing optical activity is when the horizontal axes coincide; concerning the optical activity, this reduces to the previously considered single-wall case [Eq. (11)].

Note that among the ZA combinations, there are incommensurate tubes with symmetries $\mathbf{S}_4$ and $\mathbf{D}_{2n}$, with a nontrivial tensor A, which are still inactive since the only candidate for the optical axis is the z axis, while $a_{zz}=0$. The same argument has been used in several previously discussed cases to eliminate some specific arrangements of the optical axes.

In recent effective-medium calculations of the optical properties of the aligned carbon nanotubes,[20] the dielectric constants of graphite ($\varepsilon_\parallel$ and $\varepsilon_\perp$ for the directions parallel and perpendicular to the graphite sheets, respectively) are transferred to cylindrical multishells, assuming that the nanotube is locally similar to graphite. That is, instead of Eq. (12), the most general form of the dielectric tensor is Eq. (15), with $\varepsilon_{zz}=\varepsilon_\perp$ and ε_{xx}, ε_{xy}, and ε_{yy} depending on both graphite dielectric constants. This further specifies the geometry of the optical axes in the following low-symmetry cases (otherwise, the restrictions imposed by the line-group symmetry of the nanotube are more severe). That is, the optical axes of tubes with symmetries $\mathbf{T}$ and $\mathbf{C}_1$ will lie in the xy plane, or this plane will bisect them [Fig. 3(d) or 3(c), respectively, with independent α and β]. Concerning the tubes with symmetry $\mathbf{TD}_1$ or $\mathbf{D}_1$, if the optical axes are bisected by the yz plane, they lie in one of the other two coordinate planes; thus only the two limiting cases of Fig. 3(b) arise: with the same angle and sense of rotation, the axes are either

in the xy plane [Fig. 3(d)] or the yz plane [Fig. 3(c)]. Analogously, for the tubes with $\mathbf{TC}_{1v}$, $\mathbf{T}_c$, or $\mathbf{C}_{1v}$ symmetry, the axes lie either in the xy or yz plane, while the σ_v plane bisects them; again one of the two limiting cases of Fig. 3(b) is relevant: with $\alpha=-\beta$, the axes' plane is either the horizontal [Fig. 3(d)] or the vertical one [Fig. 3(c)].

Finally, it should be noted that, although the line groups are related exclusively to infinite quasi-1D systems, the results presented in this section correspond equally well to both infinite- and finite-length nanotubes, since the dielectric and optical tensors are determined by an isogonal group only. On the other hand, the optical activity should continuously diminish as the tube diameter increases, approaching the inactive 2D graphene sheet.

IV. POTENTIALS IN NANOTUBES

Potentials produced by a single-wall nanotube must be invariant under the transformations of its symmetry group $\mathbf{L}$. This means that the potential $V(\mathbf{r})$ is a spatial function obeying

$$V(\mathbf{r})=V[(P|t)^{-1}\mathbf{r}] \tag{20}$$

for each element $(P|t)$ of $\mathbf{L}$ acting according to Eq. (1). In the forthcoming analysis this property is used to obtain quite restrictive conditions on the form of V. Since the invariance under the generators implies the invariance under the whole group, Eq. (20) should be inspected only for the generators of $\mathbf{L}$ to find the independent conditions. The single-wall nanotubes will be treated explicitly, but hints for generalization to the multiwall ones will be given too.

The translational and rotational symmetries of the tube, generated by $(I|a)$ and C_n, immediately enable one to obtain the Fourier expansion over the cylindrical coordinates φ and z:

$$V(\mathbf{r})=\sum_{K,M=-\infty}^{\infty}\alpha_K^M(\rho)e^{\imath nM\varphi}e^{\imath(2\pi/a)Kz}. \tag{21}$$

To incorporate the whole subgroup $\mathbf{L}^{(1)}$, the screw axis generator $(C_q^r|(n/q)a)$ should be employed. Relation (20) becomes $V(\rho,\varphi,z)=V[\rho,\varphi-(2\pi/q)r,z-(n/q)a]$. When applied to Eq. (21), this helical group restricts the sum only to the terms, with $Mr+K$ being multiple of q/n:

$$V(\mathbf{r})=\sum_{\substack{K,M=-\infty\\ Mr=-K \bmod\left(\frac{q}{n}\right)}}^{\infty}\alpha_K^M(\rho)e^{\imath nM\varphi}e^{\imath(2\pi/a)Kz}. \tag{22}$$

For the zigzag and armchair tubes $q=2n$ and $r=1$, and the restriction $M=-K \bmod(2)$ reduces the sum to the terms with K and M of the same parity:

$$V(\mathbf{r})=\sum_{\substack{M,K=-\infty\\ \text{odd}}}^{\infty}\omega_K^M(\rho)e^{\imath Mn\varphi}e^{\imath K(2\pi/a)z}+\sum_{\substack{M,K=-\infty\\ \text{even}}}^{\infty}\epsilon_K^M(\rho)e^{\imath Mn\varphi}e^{\imath K(2\pi/a)z}. \tag{23}$$

Additional symmetries are manifested as relations between the coefficients $\alpha_K^M(\rho)$ in Eq. (22). The invariance under the horizontal U axis reads $V(\rho,\varphi,z)=V(\rho,-\varphi,-z)$, giving $\alpha_K^M(\rho)=\alpha_{-K}^{-M}(\rho)$; thus the most general potential of the chiral single-wall nanotube is

$$V(\mathbf{r})=\sum_{\substack{K,M=0\\ Mr=-K \bmod(q/n)}}^{\infty}\pi_K^M(\rho)\cos\left(\frac{2\pi}{a}Kz+nM\varphi\right)+\sum_{\substack{K,M=0\\ Mr=K \bmod(q/n)}}^{\infty}\mu_K^M(\rho)\cos\left(\frac{2\pi}{a}Kz-nM\varphi\right). \tag{24}$$

As for the zigzag and armchair tubes, potential (23) is invariant under σ_v and U. For further purposes σ_v is considered at first; manifesting as the requirement $V(\rho,\varphi,z)=V(\rho,-\varphi,z)$, this gives $\omega_K^M=\omega_K^{-M}$ and $\epsilon_K^M=\epsilon_K^{-M}$, and the potential (the most general one for the line group $\mathbf{T}_{2n}^1\mathbf{C}_{nv}$, of the eighth family)

$$V(\mathbf{r})=\sum_{\substack{K=-\infty\\ \text{odd}}}^{\infty}\sum_{\substack{M=1\\ \text{odd}}}^{\infty}\omega_K^M(\rho)\cos(Mn\varphi)e^{\imath K(2\pi/a)z}+\sum_{\substack{K=-\infty\\ \text{even}}}^{\infty}\sum_{\substack{M=0\\ \text{even}}}^{\infty}\epsilon_K^M(\rho)\cos(Mn\varphi)e^{\imath K(2\pi/a)z}. \tag{25}$$

Including the U axis as in Eq. (24), the general zigzag and armchair potentials are obtained:

$$V(\mathbf{r})=\sum_{\substack{M,K=1\\ \text{odd}}}^{\infty}\omega_K^M(\rho)\cos\left(\frac{2\pi}{a}Kz\right)\cos(Mn\varphi)+\sum_{\substack{M,K=0\\ \text{even}}}^{\infty}\epsilon_K^M(\rho)\cos\left(\frac{2\pi}{a}Kz\right)\cos(Mn\varphi). \tag{26}$$

Note that due to the implicitly encountered σ_h invariance, all the terms are invariant when the z axis is reversed, in contrast to the chiral case.

The obtained potentials can be further specified. When a Taylor expansion of $\alpha_K^M(\rho)$ is performed, the sum of terms with the same order in ρ is an invariant polynomial of the line group. Therefore, this is a polynomial over the integrity basis of the line group,[21] with a very restricted form. As for the translationally periodic multiwall tubes, the method described can be applied, with analogous results. A different situation occurs with nanotubes having incommensurate components. They have only point-group symmetries, acting on the coordinates according to the homogeneous rules. Instead of the Fourier expansions in φ and z, the total Taylor expansion is considered, with terms being invariant polynomials in all the coordinates. So only the Molien functions and the integrity bases for the point groups are to be used.[22] These topics will be considered elsewhere in detail, while in the rest of this section some important implications of the presented results will be derived. For simplicity, zigzag and armchair nanotubes will be considered.

The separation of even and odd terms characterizes potentials (23), (25), and (26) related to the screw axis $\mathbf{T}_{2n}^1$ of the zigzag and armchair tubes. In addition to the terms indepen-

dent of z, in the even part there are terms with translational periods that are fractions of $a/2$. The periods of the odd harmonics are odd fractions of the original period a of the tube. All the terms with the periodicity of the tube, i.e., with $K=1$, have a nontrivial rotational periodicity $2\pi/Mn$. Of course, this reveals the influence of the helical nature of the tube on its physical properties. For example, the constant electric field along the tube axis breaks the z-reversal symmetries, lowering the symmetry group to $\mathbf{T}^1_{2n}\mathbf{C}_{nv}$, and the resulting current density is given by Eq. (25). Therefore, either the local-density variations are due only to the harmonics with the periods being even fractions of $a/2$, or there are chiral current components; this can be experimentally tested. In fact, all the terms with $M,K\neq 0$ also give this interesting possibility.

Finally, possible relative positions of a double-wall tube consisting of zigzag or armchair components will be discussed. Their mutual interaction can be considered as the sum of the potentials that the atoms of the second tube $[(n',0)$ or $(n',n')]$ experience in field (26) produced by the first tube $(n,0)$ or (n,n). The potential of the whole second nanotube becomes $\Sigma_{t=-\infty}^{\infty}\Sigma_{s=0}^{n'}\Sigma_{u=0}^{1}V(\mathbf{r}_{tsu})$. This sum depends on the relative positions of the single-wall components, which are parametrized by the angle φ_0 and the height z_0 between their U axes. With the help of Eqs. (6) and (7) the potential $V_n^{n'}$ over a single atom can be calculated. For ZA and AZ tubes, the obtained potential is constant, i.e., independent of the relative position of the single-wall components. This is a natural consequence of the incommensurability of the zigzag and armchair tubes. That is, two coaxial incommensurate helices pass through all the possible mutual positions, independently of their initial points (the tube is considered to be long enough), and none of their relative spatial positions is singled out. Thus no energy is required for relative coaxial translations and rotations of the components, and this is manifested as the obtained constant potential. In the cases of ZZ and AA tubes one finds [the constants ω_K^M and ϵ_K^M are the values of the coefficients in the radius $\rho=D'/2$ of the second tube and $N=\mathcal{G}(n,n')$]

$$V_n^{n'}=\sum_{\substack{M,K=1\\ \text{odd}}}^{\infty}\omega_K^M\cos\left(\frac{2\pi}{a}Kz_0\right)\cos\left(\frac{nn'}{N}M\varphi_0\right)\sin^2\left(\frac{\pi nn'}{2N^2}\right)+\sum_{\substack{M,K=1\\ \text{even}}}^{\infty}\epsilon_K^M\cos\left(\frac{2\pi}{a}Kz_0\right)\cos\left(\frac{nn'}{N}M\varphi_0\right). \tag{27}$$

Note that the odd terms appear only in the ''odd'' case (Table I), with the symmetry group $\mathbf{T}^1_2\mathbf{C}_N$ in a general position. The minima of this potential single out the preferred relative positions of the tubes. The importance of such an analysis stems from the expected dependence of the properties of the tube on the relative positions of the components, as illustrated in the discussion on the optical activity. For further considerations, some assumption on the realistic forces between the components is needed. Here we note only that an absolute extremal point of the potential is $\varphi_0=z_0=0$, i.e., the position of the coincident U axis of the components. Thus maximal symmetry positions are preferred if the forces are attractive.

V. CONCLUDING REMARKS

All the geometrical symmetries of the nanotubes are found. In addition to the rotations, translations, and screw axes observed previously, the single-wall tubes always possess horizontal rotational axes; the zigzag and armchair tubes have mirror and glide planes in addition. Thus the full symmetry group is $\mathbf{T}^r_q\mathbf{D}_n$ for single-wall chiral tubes and $\mathbf{T}^1_2\mathbf{D}_{nh}$ for zigzag and armchair ones. The parameters q and r of the helical group are found in a simple and closed form. Since $2\pi/q$ is the angle of the minimal rotation (combined with fractional translation) performed by the symmetry group, the order of the principal axis of the isogonal group is q and is always even. Moreover, $2q$ is the number of the carbon atoms in the elementary translational cell of the tube. Let us mention here that the different tubes cannot have the same symmetry parameters q, r, n, and a. This profound property means that the line group is sufficient to reconstruct the tube [as demonstrated by (6)], i.e., that the symmetry completely determines the geometry and all consequent characteristics of the nanotube. The symmetries of the multiwall tubes are quite diverse: depending on the type of the single-wall components and their arrangements, all the line and axial point groups emerge: armchair and zigzag tubes can be combined to make a prototype for any line or axial symmetry group. This immediately shows that the properties of the nanotubes may vary greatly, depending not only on the single-wall constituents, but also on their mutual positions.

There are many physical properties based on symmetry, and the presented classification of the nanotubes according to their symmetry can be widely exploited. The most familiar consequence of symmetry, the special forms of the tensors related to the characteristics of the system, depends on the isogonal group. The tensors of the dielectric permeability ε and optical activity A are studied. It is demonstrated that most of the nanotubes are optically active. More important seems to be the fact that there are many special conformations of single-wall and multiwall tubes, with quite specific manifestations of the activity to be mentioned here: one and two optical axes in various positions with respect to the tube, the activity not accompanied by the optical isomers; the cooperative activity of the inactive single-wall tubes; and the inactive tubes with vanishing and nonvanishing optic tensors. Thus the results may be used to propose how to construct a large class of possibly interesting optic devices by fine nanotube synthesis only. Also, they can be valuable in the experimental identification of nanotubes.[23]

The same study revealed a subtle interrelationship of the properties of graphite layers and nanotubes. Due to the isogonal group $\mathbf{D}_{6h}$ of the honeycomb lattice, the symmetry arguments alone suffice to prevent the optical activity of graphite. Although only a few of these symmetries remain in the nanotube's line group, its isogonal point group is larger, because some of the honeycomb translations contribute to it. Nevertheless, except in the special cases of zigzag and armchair tubes, the activity is allowed, but the general form of the dielectric tensor ε is more restrictive than in graphite.

Further, the symmetry can be used to find good quantum numbers. To begin with single-wall nanotubes, the translational periodicity is reflected in the conserved quasimomentum k, taking the values from the 1D Brillouine zone

$(-\pi,\pi]$, *or its irreducible domain*[24] $[0,\pi]$. *Also, the z* component of the quasiangular momentum m is the quantum number caused by the symmetry of the principal rotational axis; it takes on the integer values from the interval $(-n/2,n/2]$, and characterizes the nanotube quantum states. The parity with respect to reversal of the z axis, induced by the horizontal rotational axis U, is the last quantum number common to all the single-wall tubes. Even and odd states with respect to this parity are conventionally denoted by $+$ and $-$. For the zigzag and armchair tubes there is, in addition, vertical mirror plane parity, introducing the quantum numbers A and B, to distinguish between the even and odd states (the parity with respect to the horizontal mirror plane is dependent on the above discussed U and σ_v parities $\pm$ and A/B). Concerning the multiwall tubes, m is again a quantum number. Again, z-reversal and vertical mirror parities may appear, depending on the concrete symmetry of the nanotube. Nevertheless, tubes with incommensurate components are not periodic, and in such cases the quasimomentum k is not an appropriate quantum number; it may be an interesting experimental question whether the approach of modulated systems can be applied to restore this quantity. The simple criterion of commensurability of the single-wall tubes is derived: they have the same $\mathcal{R}$, and $\sqrt{qq'/nn'}$ is an integer. The involved symmetry parameters q and n are discrete, allowing an exact experimental check of commensurability.

The enumerated quantum numbers may be used to discuss and predict many characteristics of the nanotubes, but the most sophisticated approach to classification and properties of different quantum states is based on the irreducible representations of the corresponding line[25,26] and point groups. Let us point out that these representations are labeled by the derived quantum numbers. The most exhaustive possible information on selection rules, comprising the conservation of quantum numbers, for processes in the nanotubes has became available[27] after the full line (or point) group symmetry was established.

The dimension of an irreducible representation equals the degeneracy of the corresponding energy level. For periodic tubes, the degeneracy of the energy bands is at most fourfold; nevertheless, if the time-reversal symmetry of the (spin-independent) Hamiltonian is encountered, the maximal degeneracy is eightfold.[28] Further, the possible degeneracies are only twofold, fourfold, and eightfold. As for multiwall nanotubes with incommensurate components, the dimensions of the irreducible representations of the axial point groups are one, two, and (if the time-reversal symmetry is included) four, showing the possible degeneracies of the energy levels. Note that the maximal of the enumerated degeneracies (eightfold and fourfold) is not possible for tubes containing at least one chiral single-wall component. Moreover, the degeneracy of the multiwall tube in the general position of its component is at most twofold, which is caused by the time-reversal symmetry exclusively.

Also, the lattice dynamics can be studied. As mentioned above, the entire single-wall tube can be obtained from its arbitrary atom by the action of the elements of its symmetry group [Eq. (8)]; in group-theoretical language, this means that the whole nanotube is a single orbit of this group,[8] and the orbit is a_1 for the chiral tube, b_1 for the zigzag tube, and d_1 for the armchair tube.[29] Thus the normal modes (phonons) are already classified.[26] The dynamical representation of the chiral tube is decomposed into the following irreducible components [the summation over k is over the interval $(0,\pi)$; in the primed sum m takes integer values from $(0,n/2)$, otherwise from $(-n/2,n/2]$; the components with $m=n/2$ appear only for n even]:

$$D^{\mathrm{dyn}}_{\mathrm{chiral}}=3({}_oA_o^+ + {}_oA_o^- + {}_\pi A_o^+ + {}_\pi A_o^- + {}_oA_{n/2}^+ + {}_oA_{n/2}^- + {}_\pi A_{n/2}^+ + {}_\pi A_{n/2}^-) + 6\sum_m{}' \ ({}_\pi E_m + {}_oE_m) + 6\sum_{k,m} {}_kE_m .$$

It can be seen that all of the $6n$ vibrational bands are doubly degenerate, as anticipated. As for the zigzag and armchair tubes the corresponding decompositions are (summation in m is over integers from $(0,n)$, and in the primed sums from $[0,(n/2)]$)

$$D^{\mathrm{dyn}}_{\mathrm{zigzag}}=2({}_oA_o^+ + {}_oA_o^- + {}_oA_n^+ + {}_oA_n^- + {}_\pi E_B) + {}_oB_o^+ + {}_oB_o^- + {}_oB_n^+ + {}_oB_n^- + 4\,{}_\pi E_A$$
$$+3\sum_m ({}_oE_m^+ + {}_oE_m^-) + 2\sum_k [{}_kE_{B_o} + {}_kE_{B_n} + 2({}_kE_{A_o} + {}_kE_{A_n})] + 6\sum_m{}' \ {}_\pi G_m + 6\sum_{k,m} {}_kG_m + 3({}_\pi E_{n/2}^+ + {}_\pi E_{n/2}^-),$$

$$D^{\mathrm{dyn}}_{\mathrm{armchair}}=2({}_oA_o^+ + {}_oB_o^+ + {}_oA_n^+ + {}_oB_n^+) + {}_oA_o^- + {}_oB_o^- + {}_oA_n^- + {}_oB_n^- + 3({}_\pi E_A + {}_\pi E_B)$$
$$+6\sum_{k,m} {}_kG_m + 3\sum_k ({}_kE_{A_o} + {}_kE_{B_o} + {}_kE_{A_n} + {}_kE_{B_n}) + \sum_m (4\,{}_oE_m^+ + 2\,{}_oE_m^-) + 6\sum_m{}' \ {}_\pi G_m + 3({}_\pi E_{n/2}^+ + {}_\pi E_{n/2}^-).$$

Analogous data can be directly found for each nanotube. This classification can be used to simplify calculation of the vibrational bands;[30] the obtained bands are automatically labeled by the symmetry-based quantum numbers, meaning that Raman and incommensurate spectra can be directly extracted by the selection rules. Note, in this context, that the Jahn-Teller theorem is proved both for point and line groups.[26]

The results of Sec. IV enable us to generalize the Bloch theorem to the line-group symmetries of the single-wall nanotubes:[6] multiplying these invariant functions by the matrix elements of the corresponding irreducible representation,

all the quantum states and covariant functions can be obtained. On the other hand, many of the nanotube properties can be understood on the basis of these potentials. The mutual independence of the incommensurate ideal infinite coaxial tubes is an interesting result, that should be understood due to their weak coupling in realistic cases. The relative arrangement of two coaxial single-wall tubes is sharply reflected by the tensor properties of the tubes, as illustrated in Sec. III. In this context, the discussion on the preferred positions, being briefly described, should be important for applications to nanotubes, as well as the proposed possibility of the chiral currents. The fields produced by such currents could also be used for tube identification.

ACKNOWLEDGMENTS

We are grateful to Dr. I. Božović (OXXEL GmbH, Bremen) and Dr. G. Biczó (Central Research Institute for Chemistry, Budapest), who brought this subject to our attention. Also, we thank Dr. R. Kostić (Institute of Physics, Beograd) for some remarks.

*Electronic address: yqoq@afrodita.rcub.bg.ac.yu

[1] S. Iijima, Nature (London) **354**, 56 (1991).
[2] M. S. Dresselhaus (unpublished).
[3] M. S. Dresselhaus, G. Dresselhaus, and P. C. Eklund, *Science of Fullerenes and Carbon Nanotubes* (Academic, San Diego, 1998).
[4] M. S. Dresselhaus, G. Dresselhaus, and R. Saito, Phys. Rev. B **45**, 6234 (1992).
[5] N. Hamada, S. Sawada, and A. Oshiyama, Phys. Rev. Lett. **68**, 1579 (1992).
[6] C. T. White, D. H. Robertson, and J. W. Mintmire, Phys. Rev. B **47**, 5485 (1993).
[7] R. A. Jishi, L. Venkataraman, M. S. Dresselhaus, and G. Dresselhaus, Phys. Rev. B **51**, 11 176 (1995).
[8] I. Milošević, R. Živanović, and M. Damnjanović, Polymer **38**, 4445 (1997).
[9] M. Damnjanović and M. Vujičić, Phys. Rev. B **25**, 6987 (1982).
[10] I. Milošević, Phys. Lett. A **204**, 63 (1995).
[11] I. Milošević, A. Damjanović, and M. Damnjanović, in *Quantum Mechanical Simulation Methods for Studying Biological Systems*, edited by D. Bicout and M. Field (Springer-Verlag, Berlin, 1996), Chap. XIV.
[12] J. P. Elliot and P. G. Dawber, *Symmetry in Physics* (Macmillan, London, 1979).
[13] The following standard notation is used: σ_v is the vertical mirror plane, I is the 3×3 identity matrix, while a denotes the translational period. Also, C_q^r is the rotation for $2\pi r/q$ around the z axis, where $0\leqslant r<q/n$ and q/n are coprime integers. Instead of this helical group **Z**, generated by $[C_q^r|(n/q)a]$, the groups generated by $[C_q^{r_i}|(n/q)a]$, with $r_i=r+iq/n$, $i=1,\ldots,n-1$, give the same full symmetry group (Ref. 6). Among these r_i's there is at least one that is coprime with q; with this r_i, it is obvious that the set $[C_q^{tr_i}|t(n/q)a]$ contains the rotations for all the multiples of $2\pi/q$ (followed by some translations).
[14] T. Vuković, Ph.D. thesis, University of Beograd, 1999.
[15] W. A. de Heer *et al.*, Science **268**, 845 (1995).
[16] Y. Saito, T. Yoshikawa, S. Bandow, M. Tomita, and T. Hayashi, Phys. Rev. B **48**, 1907 (1993).
[17] R. Saito, M. Fujita, G. Dresselhaus, and M. Dresselhaus, Appl. Phys. Lett. **60**, 2204 (1992).
[18] L. D. Landau and E. M. Lifshitz, *Electrodynamics of Continuous Media* (Pergamon, Oxford, 1963).
[19] S. Tasaki, K. Maekawa, and T. Yamabe, Phys. Rev. B **57**, 9301 (1998). The third-rank tensor $\Gamma=(\gamma_{ijk})$ used in that paper is related to the tensor A by $(\omega/c)\gamma_{ijk}=\Sigma_l\varepsilon_{ijl}a_{lk}$ (ω is the frequency of the incoming light, c the light speed in vacuum, and ε_{ijk} the Levi-Civita tensor.
[20] F. J. García-Vidal, J. M. Pitarke, and J. B. Pendry, Phys. Rev. Lett. **78**, 4289 (1997).
[21] T. Muković, I. Milošević, and M. Damnjanović, Phys. Lett. A **216**, 307 (1996).
[22] J. Patera, R. T. Sharp, and P. Winternitz, J. Math. Phys. **19**, 2362 (1978); A. G. McLellan, J. Phys. C **7**, 3326 (1974); J. Killinback, *ibid.* **5**, 2497 (1972).
[23] X. Wan, J. Dong, and D. Y. Xing, Phys. Rev. B **58**, 6756 (1998).
[24] S. L. Altmann, *Band Theory of Solids. An Introduction from the Point of View of Symmetry* (Clarendon Press, Oxford, 1991).
[25] I. Božović, M. Vujičić, and F. Herbut, J. Phys. A **11**, 2133 (1978); I. Božović and M. Vujičić, J. Phys. A **14**, 777 (1981).
[26] I. Milošević and M. Damnjanović, Phys. Rev. B **47**, 7805 (1993).
[27] I. Božović, N. Božović, and M. Damnjanović, J. Phys. A **18**, 923 (1985).
[28] M. Damnjanović, I. Milošević, and M. Vujičić, Phys. Rev. B **39**, 4610 (1989); M. Damnjanović and I. Milošević, *ibid.* **43**, 13 482 (1991).
[29] Since the whole zigzag and armchair nanotubes are produced by the action of the subgroup $\mathbf{T}_{2n}^1\mathbf{D}_n$ on an arbitrary atom, each atom is invariant under one (nontrivial) transformation of the full symmetry group (the stabilizers of the atoms are nontrivial). For example, the starting atom is invariant under the point group $\mathbf{C}_{1v}$ in the zigzag tube, and under $\mathbf{C}_{1h}$ in the armchair tube.
[30] A. Charlier, E. Mc Rae, M. F. Charlier, A. Spire, and S. Forster, Phys. Rev. B **57**, 6689 (1998).